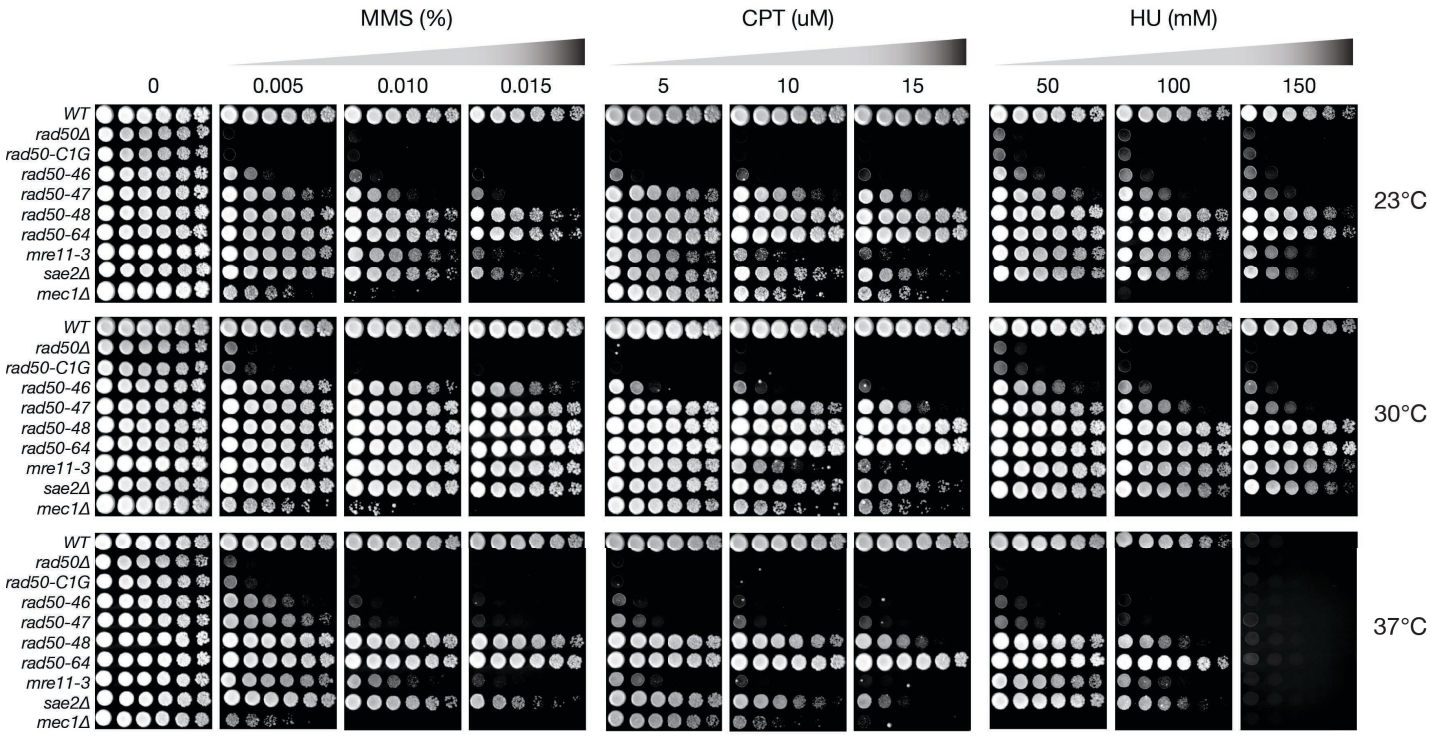


**Figure S1, related to Figure 1**. **S-phase clastogen sensitivity of *rad50$^{hook}$* at different temperatures**. Cell survival on plates containing the indicated concentrations of MMS, CPT or HU. 5-fold serial cell dilutions were spotted and plates were incubated at 30°C, 23°C or 37°C. Allele names refer to the following mutations: *rad50-C1G (C687G), rad50-46 (S685R Y688E), rad50-47 (L689R), rad50-48 (S685R Y688R), rad50-64 (S685E Y688R), mre11-3 (H125L D126V*). The *mec1Δ* strain also contained *sml1Δ*.

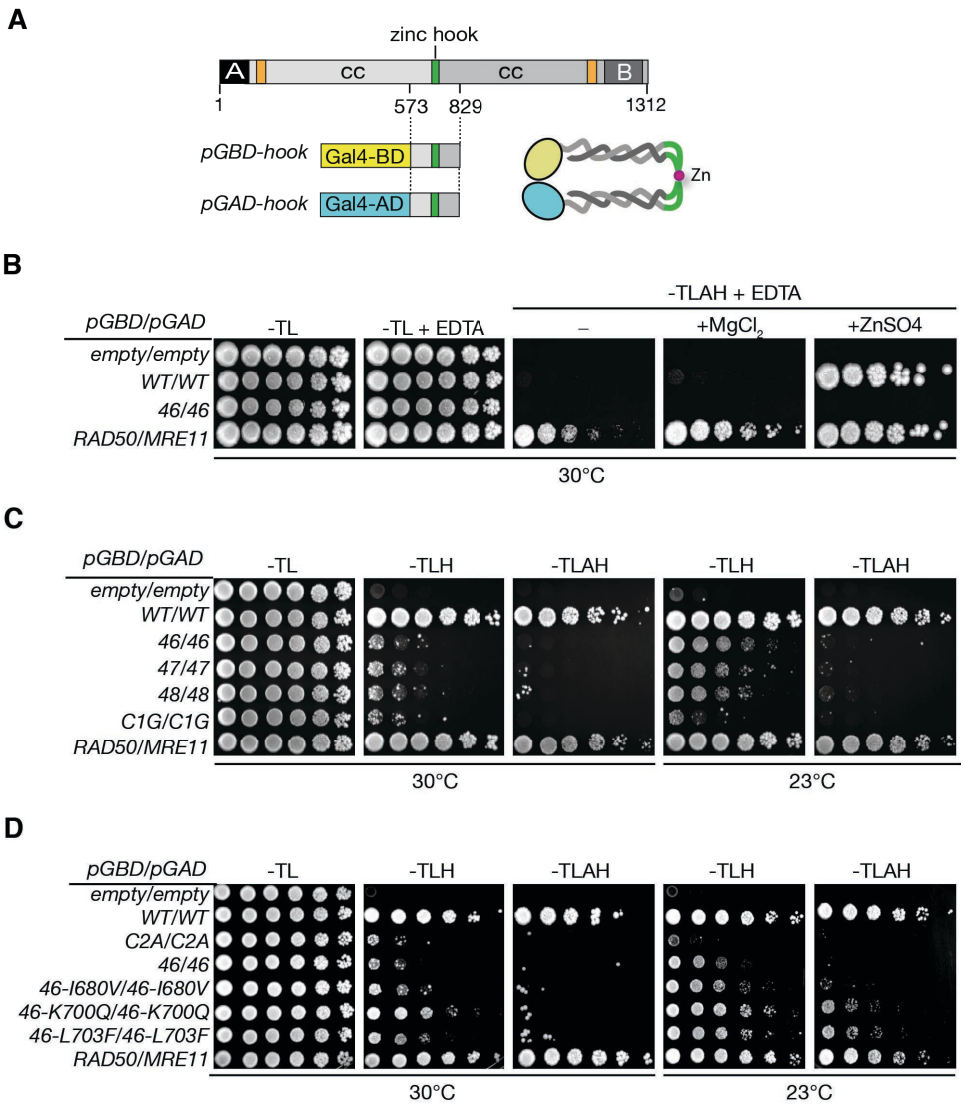


**Figure S2, related to Figure 2 and Figure 7. Rad50 hook dimerization by yeast-2 hybrid analysis. A.** Rad50 peptides containing the hook and flanking coiled coil domain (residues 573-829) were co-expressed as either a fusion protein with the Gal4 -Binding Domain (BD, *pGBD*; *TRP1*) or with the Gal4 - Activation Domain (AD, *pGAD; LEU2*) in a *rad50Δ* yeast-2 hybrid reporter strain. Cells were grown on media lacking tryptophan and leucine (-TL) to assure plasmid retention. Reporter activation was monitored by growth on plates lacking also histidine (-TLH) or histidine and adenine (-TLHA). **B.** Reporter activation is zinc dependent. EDTA (0.5 mM) and $MgCl_2$ or $ZnSO_4$ (both 1 mM) were included in plates as indicated. The Rad50-Mre11 interaction (full length proteins) served as a positive control (bottom lane in B-D). Plates were incubated at 30°C. **C**. Lack of reporter activation in strains expressing various *rad50*$^{hook}$ mutant (*rad50-46, rad50-47, rad50-48* or *rad50-C1G*) constructs irrespective of incubation temperature (30°C or 23°C, as indicated). **D.** *rad50-46* hook peptides containing *rad50-46* hook suppressors mutations (I680V, K700Q or L703F) failed to significantly rescue reporter activation. C2A = *rad50-C690A*.

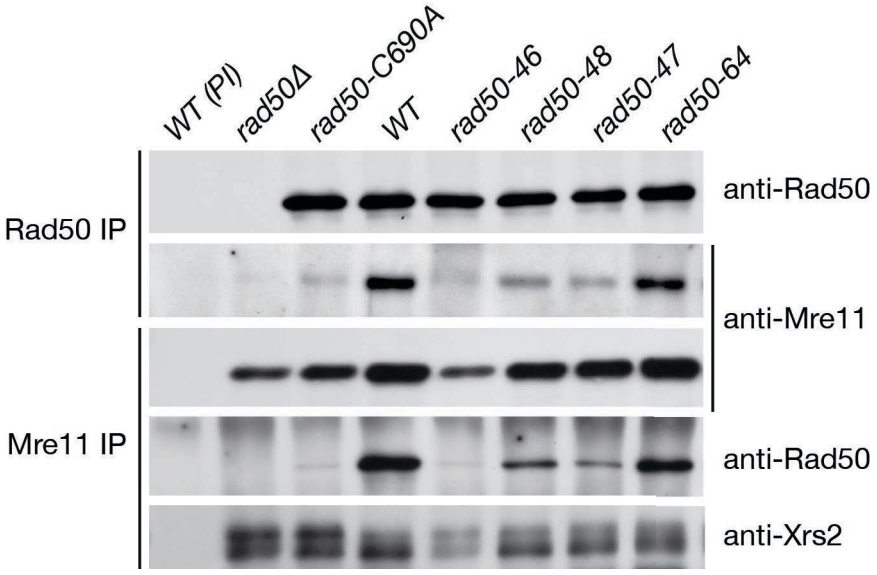


**Figure S3, related to Figure 3**. **Mre11 complex integrity in *rad50*$^{hook}$ mutants**.
Mre11 complex integrity in wild-type and *rad50*$^{hook}$ assessed by co-immuno-precipitation with Rad50 or Mre11 antibodies (Rad50-IP or Mre11-IP) and western blot (anti-Rad50, anti-Mre11 or anti-Xrs2). Pre-immune antibodies (PI) were included as negative controls.

**A**

Short (2 hours) HO-induction

| Genotype | imprecise | NHEJ events |
|---|---|---|
| *WT* | 0/40 | accurate |
| *rad50Δ* | 10/33 (30.3%) | ΔACA (7),ΔCAG (1), ΔGC (1) ΔCGCAACAG (1) |
| *rad50-46* | 12/60 (20%) | ΔACA (7), ΔAC (2), ΔGCA (1), mut (2) |
| *rad50-47* | 5/33 (15.2%) | ΔACA (3), ΔA (1), ΔC (1) |
| *rad50-48* | 2/33 (6.1%) | ΔACA (2) |

**B**

Persistent HO-induction

| Genotype | Total | NHEJ events |
|---|---|---|
| *WT* | 42 | +CA (30), +CAA (2), +ACA (1), +AA (1), ΔA (3), ΔC (2), ΔACA (1),ΔGTA (1), ΔGCAACAC (1) |
| *rad50Δ* | 28 | ΔACA (4), ΔCA (16),ΔA (2), ΔAG (1), ΔCAACAG (1), ΔAACAGTAT (2), none (2) |
| *rad50-46* | 82 | +CA (1), +A (1), ΔACA (70), ΔAC (2), ΔGC (2), ΔA (1), ΔC (1), ΔGCAAC (1), others (1), mut (2) |
| *rad50-47* | 45 | +CA (4), +AC (2), ΔACA (22), ΔAC (1), ΔGC (1), ΔA (5), ΔCAACAG (2), mut (5), ΔACA+mut (2) |
| *rad50-48* | 42 | +CA (9), +ACA (2), +AC (9), ΔACA (9), ΔGCA (1), ΔGC (2), ΔC (4), ΔA (4), none (2) |
| *rad50S* | 30 | +CA (9), +ACA (2), ΔACA (9), ΔGCA (1), ΔCAG (1), ΔGC (1), ΔCA (1), ΔC (1), ΔAGTATAATTTTATAAACC (1), +CA+ΔC (1), mut (3) |

| Genotype | Total | Insertion | Deletions | P-Mutation | Others | >4nt change |
|---|---|---|---|---|---|---|
| *WT* | 42 | 34 (81%) | 8 (19%) | 0 | 0 | 1 (2%) |
| *rad50Δ* | 28 | 0 | 26 (93%) | 0 | 2 (7%) | 3 (11%) |
| *rad50-46* | 82 | 2 (4%) | 77 (94%) | 2 (2%) | 3 (4%) | 1 (1%) |
| *rad50-47* | 45 | 6 (13%) | 31 (69%) | 5 (11%) | 2 (4%) | 2 (4%) |
| *rad50-48* | 42 | 20 (48%) | 20 (48%) | 0 | 2 (4%) | 0 |
| *rad50S* | 30 | 11 (37%) | 15 (50%) | 3 (10%) | 1 (3%) | 1 (3%) |

**Figure S4, related to Figure 3**. **NHEJ repair junctions of survivor colonies.**
**A.** NHEJ events upon short HO-induction (2 hours) of survivors shown in Figure 3D. Numbers of imprecise NHEJ events versus total numbers of NHEJ junctions sequenced are given. Imprecise NHEJ events were either deletions (Δ) or point mutations (mut) and are listed. No error prone NHEJ events were found among wild-type survivors. **B.** NHEJ events of survivors (Figure 3E) following persistent HO-induction. The top panel lists all mutational events, either insertions (+), deletions (Δ) or point mutations (mut). “None” indicates that the HO-site was unaltered. The lower panel summarizes the frequency of the categorized events for each genotype. P-Mutation, point mutation; Others, no or more complex mutations of the HO-site (insertion and deletions >4 nt in size).

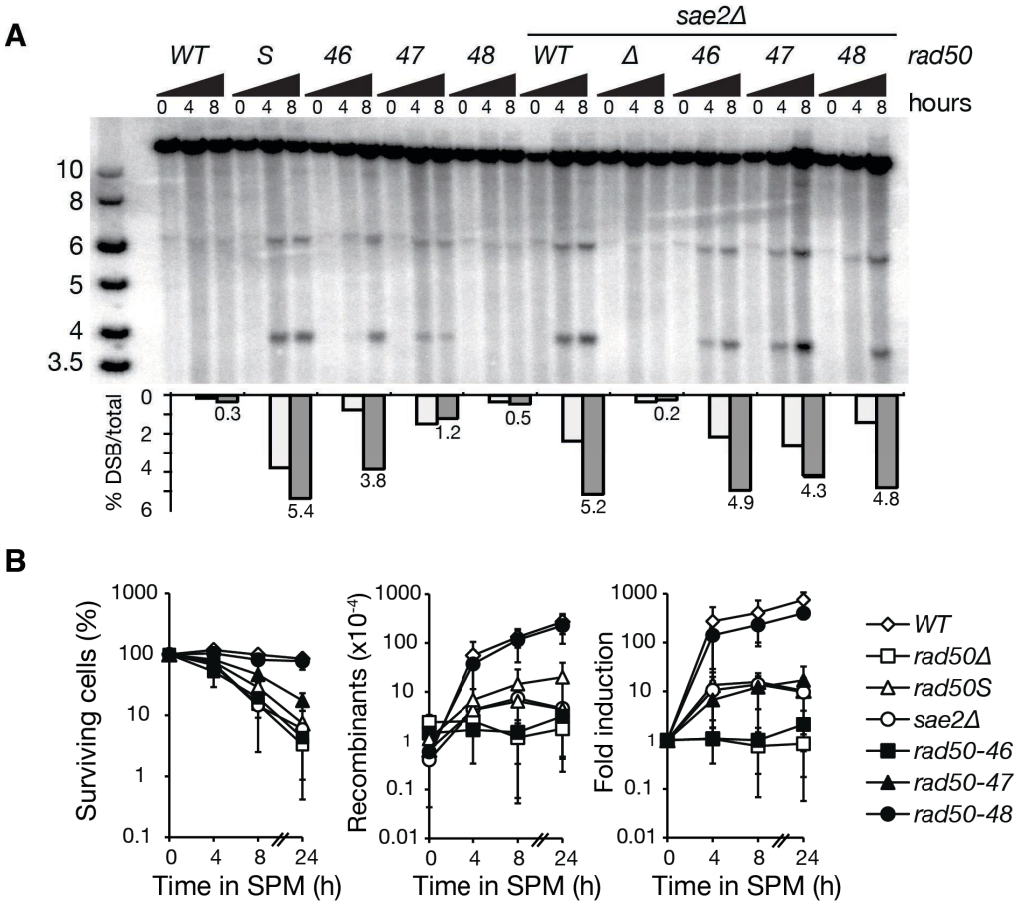


**Figure S5, related to Figure 5. Meiotic DSB formation at the *HIS4-LEU2* meiotic hotspot**. **A**. Cells were cultivated for 0, 4 and 8 hours in sporulation medium and meiotic DSB formation was assessed by Southern blot with a hotspot-specific probe. The genotypes from left to right are: *WT*, *rad50S*, *rad50-46*, *rad50-47*, *rad50-48*, *sae2Δ*, *rad50Δ sae2Δ, rad50-46 sae2Δ, rad50-47 sae2Δ, rad50-48 sae2Δ.* Quantification of the DSB fragments (6 and 3.7 kb bands) as a fraction of total signal intensity per lane is given on bottom of the southern blot. **B**. In return-to-growth assays, recombination intermediate formed in meiosis are resolved by the mitotic DSB repair apparatus. Diploids of the indicated genotypes containing the *his4-B*/*his4-X* heteroalleles were incubated for 0, 4, 8 and 24 hours (h) in sporulation media (SPM) and plated on media without and with histidine. The percentage of surviving cells was calculated by the ratio of colonies formed on media with histidine versus the total number of cells plated (graph on the left) and the recombination frequency as numbers of colonies formed on media without versus on media with histidine (graph in the middle). The graph on the right shows the fold of meiotic recombination induction for each time point as a ratio to the recombination frequency at t=0 (normalized as 1). Error bars denote standard deviation from at least three independent experiments.

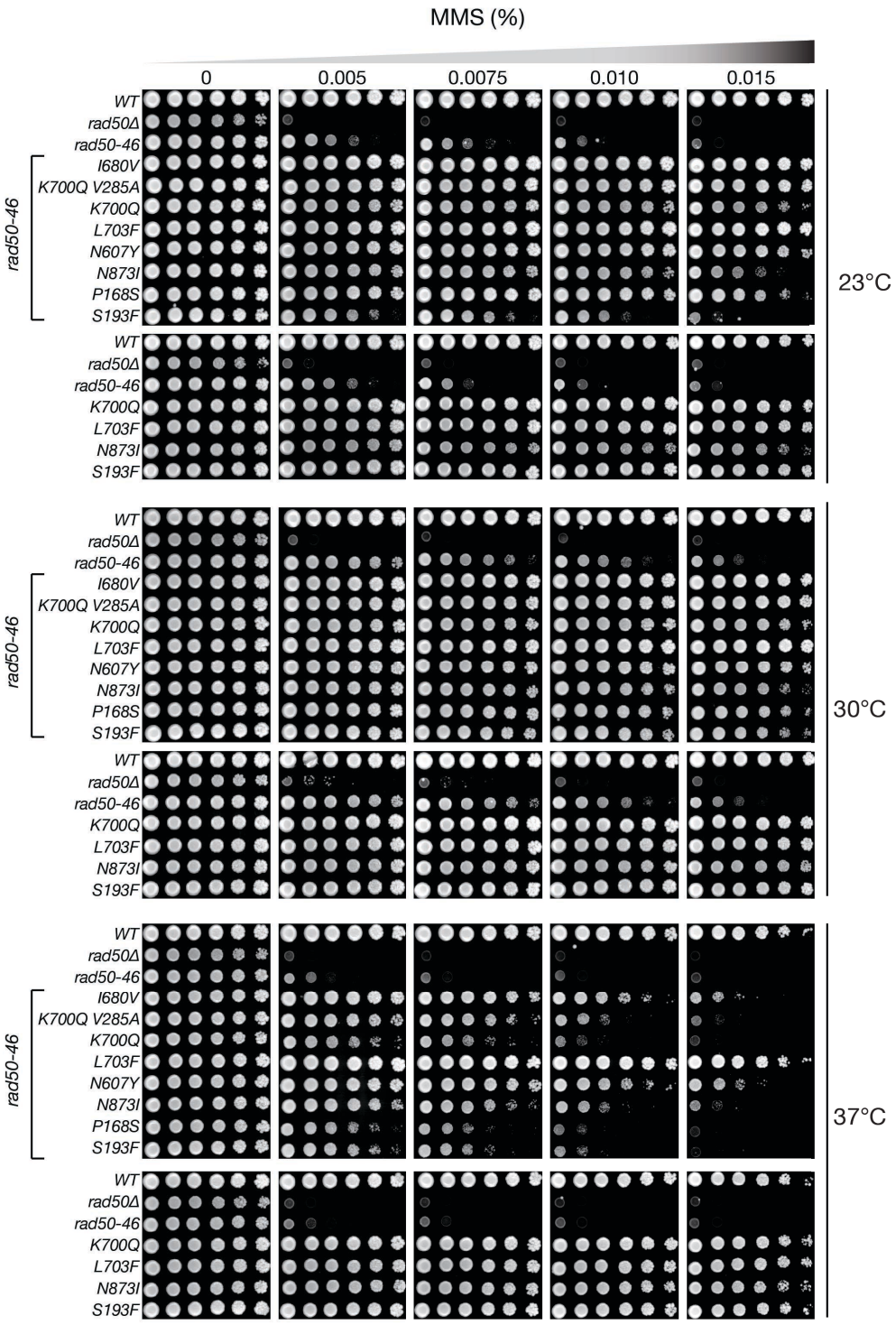


**Figure S6, related to Figure 7. Suppression of *rad50-46* MMS survival by intragenic suppressors.** Extended spot test of Figure 7B. Plates without or with the indicated concentrations of MMS were incubated at 23°C, 30°C or 37°C. Suppressors were tested in context of *rad50-46* allele or in context of the wild-type hook domain as indicated.

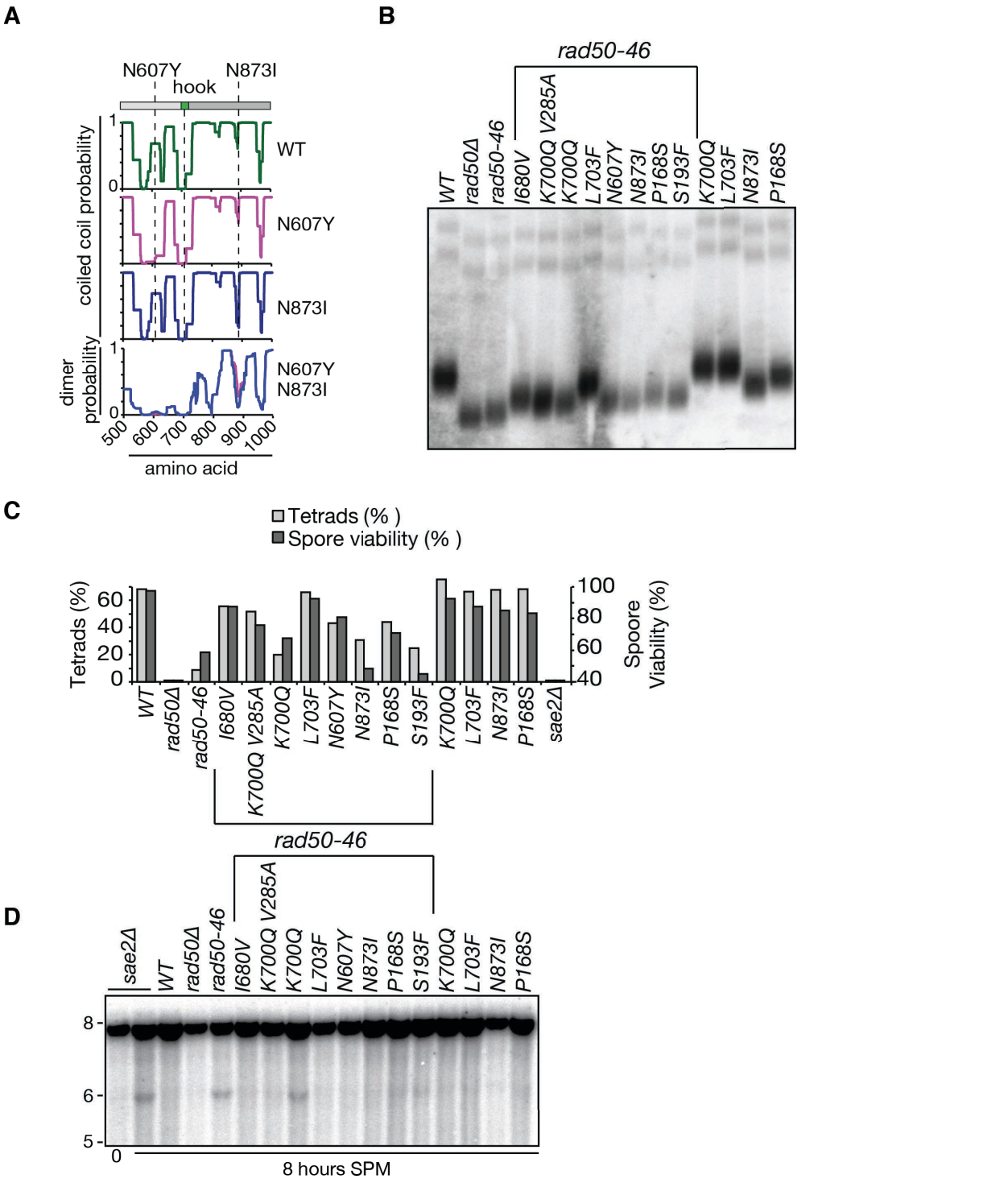


**Figure S7, related to Figure 7. Intragenic suppressors mitigate *rad50-46* telomere and meiotic defects to various extents. A.** Graphs depicting the probabilities of Rad50 WT, Rad50-N607Y and Rad50-N873I residues 500-1000 to assume a coiled coil structure (three graphs on the top) or to form coiled coil dimers (graph on bottom). Probabilities were calculated with the programs “Coil” and “MultiCoil” using a window width of 28. **B.** Telomere

lengths of *rad50-46* without and with suppressor mutants monitored by Southern blot of freshly dissected spores after 30 generations of growth. The strains labeled on top with "*rad50-46"* contain both the *rad50-46* hook allele and the indicated suppressor mutations, whereas the last four strains on the right contain only the suppressor mutations in context of a wild-type hook. **C.** Analysis of suppression of *rad50-46* meiotic defect by the various suppressor mutants. Top: W303+ *rad50Δ/Δ* diploids containing either an empty or *Ycp50-rad50* plasmid of the indicated genotypes were sporulated in liquid culture for 48 hours and for each culture the percentage of tetrad formation (by microscopy) and spore viability (by tetrad dissection) was determined. Bottom: Same cultures as above were incubated in sporulation media (SPM) for 8 hours and meiotic DSB formation at the *THR4* locus was assessed by southern blot. A band of 6.0 kb corresponding to the unresected meiotic DSB fragment was evident after 8 hours in sporulation media in *sae2Δ/Δ* and *rad50Δ/Δ Yp50-rad50-46* control strains, and to similar levels in cells containing the *Yp50-rad50-46-K700Q* plasmid, but not *Yp50-rad50-46-K700Q V285A*. Resolution of this blot was to low to unambiguously conclude if the meiotic DSB fragment might be also present at lower levels in other genotypes.

**Table S1, related to Experimental Procedures. *S. cerevisiae* strains used in this study**

Strains were in the following yeast background: **W303**$^{+}$ (*trp1-1 leu2-3,112 ura3-1 can1-100 ade2-1 his3-11,15 RAD5*), **DBY745** (*leu2-3,112 lys5 ura3-52 adel-100*) or **SK1** background (*ho::LYS2 lys2 his4::LEU2 arg4 ura3 leu2::hisG*) and only differences from this genotype are listed. Following abbreviations are used: *GAL-TEV (GAL-NLS-myc9-TEV-NLS::TRP1); KAN (KanMX4);* W303$^{+}$ (W303 *RAD5*)*. URA3* counterselected on 5-FOA is indicated with *ura3*. An asterisk (*) indicates homoalleles in diploid strains.

| Strain ID | Genotype | Background/Source | |
|---|---|---|---|
| JPY708 | *MATa WT* | W303 | Lab Stock |
| JPY1450 | *MATα rad50Δ::KAN* | W303 | Lab Stock |
| JPY2874 | *MATa rad50-46::HYG FLAG-RAD53::LEU2* | W303 | this study |
| JPY4448 | *MATa rad50-47::HYG FLAG-RAD53* | W303 | this study |
| JPY4620 | *MATα rad50-48::HYG FLAG-RAD53* | W303 | this study |
| JPY4406 | *MATa rad50-64::HYG FLAG-RAD53* | W303 | this study |
| JPY4479 | *MATa rad50-C1G::HYG FLAG-RAD53* | W303 | this study |
| JPY2879 | *MATa rad50-C2A::HYG FLAG-RAD53* | W303 | this study |
| JPY3663 | *MATa mre11-3::URA3* | W303 | Lab Stock |
| JPY2252 | *MATa sae2Δ::KAN FLAG-RAD53* | W303 | Lab Stock |
| | *MATa-inc leu2-SFA1 ade3::GAL-HO* | W303 | Aguilera |
| | *MATa-inc rad50Δ::??? leu2-SFA1 ade3::GAL-HO* | W303+ | Aguilera |
| JPY5463 | *MATa-inc rad50-46::HYG leu2-SFA1 ade3::GAL-HO* | W303+ | this study |
| JPY5465 | *MATa-inc rad50-47::HYG leu2-SFA1 ade3::GAL-HO* | W303+ | this study |
| JPY5467 | *MATa-inc rad50-48::HYG leu2-SFA1 ade3::GAL-HO* | W303+ | this study |
| JPY2422 | *MATa/α rad50Δ/Δ ade2Δn/ade2-ISceI LEU-TetR/- URA3-tetO112/- GAL-TEV::TRP1* | W303+ | this study |
| JPY2422 | *MATa/α RAD50/Δ ade2Δn/ade2-ISceI ura3-tetO112/- GAL-TEV::TRP1* | W303+ | this study |
| JPY3832 | *MATa/α rad50-46::HYG/Δ ade2Δn/ade2-ISceI URA3-tetO112/- GAL-TEV::TRP1* | W303+ | this study |
| JPY5125 | *MATa/α rad50-47::HYG/Δ ade2Δn/ade2-ISceI URA3-tetO112/- GAL-TEV::TRP1* | W303+ | this study |
| JPY5127 | *MATa/α rad50-48::HYG/Δ ade2Δn/ade2-ISceI URA3-tetO112/- GAL-TEV::TRP1* | W303+ | this study |
| JPY3765 | *MATα RAD50::HYG Δho Δhml::ADE1Δhmr::ADE1 ade3::Gal-HO* | DBY745 | this study |
| JPY3763 | *MATα rad50-46::HYG Δho Δhml::ADE1Δhmr::ADE1 ade3::Gal-HO* | DBY745 | this study |
| JPY4641 | *MATα rad50-47::HYG Δho Δhml::ADE1Δhmr::ADE1 ade3::Gal-HO* | DBY745 | this study |
| JPY4610 | *MATα rad50-48::HYG Δho Δhml::ADE1Δhmr::ADE1 ade3::Gal-HO* | DBY745 | this study |
| JPY1887 | *MATα rad50Δ mec1ΔTRP1 sml1ΔHIS3* | W303+ | this study |
| JPY1953 | *MATa rad50Δ mec1ΔHYG sml1ΔHIS3 sae2Δ FLAG-RAD53::LEU2* | W303+ | this study |
| JPY3872 | *MATa mec1ΔHYG sml1ΔHIS3 FLAG-RAD53::LEU2* | W303+ | this study |
| JPY3873 | *MATa mec1ΔHYG sml1ΔHIS3 sae2ΔKAN FLAG-RAD53::URA3* | W303+ | this study |
| JPY3848 | *MATa rad50-46::HYG mec1ΔHYG sml1ΔHIS3 FLAG-RAD53::URA3 GAL-TEV::TRP1* | W303+ | this study |
| JPY3853 | *MATa rad50-46::HYG mec1ΔHYG sml1ΔHIS3 sae2ΔKAN FLAG-RAD53::LEU2* | W303+ | this study |
| JPY5555 | *MAT? rad50-47::HYG mec1ΔHYG sml1ΔHIS3 FLAG-RAD53* | W303+ | this study |
| JPY5557 | *MAT? rad50-47::HYG mec1ΔHYG sml1ΔHIS3 sae2ΔKAN FLAG-RAD53::URA3* | W303+ | this study |
| JPY5488 | *MATa rad50-48::HYG mec1ΔHYG sml1ΔHIS3 FLAG-RAD53::LEU2* | W303+ | this study |
| JPY5492 | *MATa rad50-48::HYG mec1ΔHYG sml1ΔHIS3 sae2ΔKAN FLAG-RAD53::LEU2* | W303+ | this study |
| JPY5496 | *MATa rad50-C1G::HYG mec1ΔHYG sml1ΔHIS3 FLAG-RAD53* | W303+ | this study |
| JPY5498 | *MATa rad50-C1G::HYG mec1ΔHYG sml1ΔHIS3 sae2ΔKAN FLAG-RAD53::LEU2* | W303+ | this study |
| JPY4926 | *MATa/α RAD50::HYG/RAD50 FLAG-RAD53::URA3/FLAG-* | W303+ | this study |

| | | | |
|---|---|---|---|
| | *RAD53::URA3 GAL-TEV::TRP1/-* | | |
| JPY4925 | *MATa/α rad50Δ::KAN/RAD50 FLAG-RAD53/FLAG-RAD53::URA3* | W303+ | this study |
| JPY4617 | *MATa/α rad50-46::HYG/RAD50 FLAG-RAD53/FLAG-RAD53* | W303+ | this study |
| JPY4446 | *MATa/α rad50-47::HYG/RAD50 FLAG-RAD53/FLAG-RAD53* | W303+ | this study |
| JPY4614 | *MATa/α rad50-48::HYG/RAD50 FLAG-RAD53/FLAG-RAD53* | W303+ | this study |
| JPY4681 | *MATa/α rad50S::HYG/RAD50 sae2ΔKAN/SAE2 FLAG-RAD53/FLAG-RAD53* | W303+ | this study |
| JPY410 | *MATa/α his4B::LEU2/his4X::LEU2* | SK1 | S.Keeney |
| JPY3969 | *MATa/α rad50-46/46::HYG his4B::LEU2/his4X::LEU2* | SK1 | this study |
| JPY4639 | *MATa/α rad50-47/47::HYG his4B::LEU2/his4X::LEU2* | SK1 | this study |
| JPY4674 | *MATa/α rad50-48/48::HYG his4B::LEU2/his4X::LEU2* | SK1 | this study |
| JPY409 | *MATa/α sae2Δ/Δ his4B::LEU2/his4X::LEU2* | SK1 | this study |
| JPY3973 | *MATa/α rad50-46/46::HYG sae2Δ/Δ his4B::LEU2/his4X::LEU2* | SK1 | this study |
| JPY5245 | *MATa/α rad50-47/47::HYG sae2Δ/Δ his4B::LEU2/his4X::LEU2* | SK1 | this study |
| JPY5247 | *MATa/α rad50-48/48::HYG sae2Δ/Δ his4B::LEU2/his4X::LEU2* | SK1 | this study |
| JPY5596 | *MATa/α HIS4::LEU2-(BamHI)/his4-X::LEU2-(NgoMIV)-URA3* | SK1 | S.Keeney |
| JPY5597 | *MATa/α dmc1Δ/Δ::HYG HIS4::LEU2-(BamHI)/his4-X::LEU2-(NgoMIV)-URA3* | SK1 | this study |
| JPY5597 | *MATa/α dmc1Δ/Δ::HYG HIS4::LEU2-(BamHI)/his4-X::LEU2-(NgoMIV)-URA3* | SK1 | this study |
| JPY5649 | *MATa/α rad50S/S HIS4::LEU2-(BamHI)/his4-X::LEU2-(NgoMIV)-URA3* | SK1 | S.Keeney |
| JPY5598 | *MATa/α rad50-46/46::HYG HIS4::LEU2-(BamHI)/his4-X::LEU2-(NgoMIV)-URA3* | SK1 | this study |
| JPY5600 | *MATa/α rad50-47/47::HYG HIS4::LEU2-(BamHI)/his4-X::LEU2-(NgoMIV)-URA3* | SK1 | this study |
| JPY5599 | *MATa/α rad50-48/48::HYG HIS4::LEU2-(BamHI)/his4-X::LEU2-(NgoMIV)-URA3* | SK1 | this study |
| JPY2162 | *MATα rad50Δura3- GAL-TEV::TRP1* | W303+ | this study |
| JPY2170 | *MATα rad50Δura3- GAL-TEV::TRP1 Ycp50 (empty)* | W303+ | this study |
| JPY2171 | *MATα rad50Δura3- Ycp50-RAD50* | W303+ | this study |
| JPY6314 | *MATα rad50Δura3- Ycp50-rad50-46* | W303+ | this study |
| JPY6325 | *MATα rad50Δura3- Ycp50-rad50-46-I680V* | W303+ | this study |
| JPY6311 | *MATα rad50Δura3- Ycp50-rad50-46-K700Q V285A* | W303+ | this study |
| JPY6315 | *MATα rad50Δura3- Ycp50-rad50-46-V285A* | W303+ | this study |
| JPY6316 | *MATα rad50Δura3- Ycp50-rad50-46-K700Q* | W303+ | this study |
| JPY6321 | *MATα rad50Δura3- Ycp50-rad50-46-L703F* | W303+ | this study |
| JPY6322 | *MATα rad50Δura3- Ycp50-rad50-46-N607Y* | W303+ | this study |
| JPY6330 | *MATα rad50Δura3- Ycp50-rad50-46-N873I* | W303+ | this study |
| JPY6313 | *MATα rad50Δura3- Ycp50-rad50-46-P168S* | W303+ | this study |
| JPY6312 | *MATα rad50Δura3- Ycp50-rad50-46-S193F* | W303+ | this study |
| JPY6329 | *MATα rad50Δura3- Ycp50-rad50-K700Q* | W303+ | this study |
| JPY6327 | *MATα rad50Δura3- Ycp50-rad50-L703F* | W303+ | this study |
| JPY6331 | *MATα rad50Δura3- Ycp50-rad50-N873I* | W303+ | this study |
| JPY6333 | *MATα rad50Δura3- Ycp50-rad50-S193F* | W303+ | this study |
| JPY6210 | *MATα rad50-N873I::HYG* | W303+ | this study |
| JPY6202 | *MATα rad50-46-N873I::HYG* | W303+ | this study |
| JPY6205 | *MATa rad50-47-N873I::HYG* | W303+ | this study |
| JPY6224 | *MATα rad50-C1G-N873I::HYG* | W303+ | this study |
| JPY6296 | *MATa rad50-short coil-N873I::HYG* | W303+ | this study |
| JPY6299 | *MATα rad50- short coil+hook-N873I::HYG* | W303+ | this study |
| JPY6381 | *MATa rad50-L703F::HYG* | W303+ | this study |
| JPY6383 | *MATα rad50-C1G-L703F::HYG* | W303+ | this study |
| JPY6385 | *MATa rad50-46-L703F::HYG* | W303+ | this study |

**Table S2, related to Figure 1**. MMS sensitivity of all *rad50* hook mutants tested. The *rad50*$^{hook}$ alleles, *rad50-46*, *-47*, *-48* are highlighted. MMS survival of most other *rad50*$^{hook}$ alleles was comparable to wild-type. Two *rad50*$^{hook}$ alleles (highlighted in pink) showed MMS sensitivity comparable to *rad50Δ*. Both alleles contained the *rad50-46* and *rad50-48* mutations, respectively, but acquired an additional third mutation (C686G or N696I), rendering these alleles MMS sensitive. The single r*ad50-C686G* and *rad50-N696I* mutant alleles were indistinguishable from wild-type, suggesting that the observed MMS sensitivity was a composite effect of the triple mutants. MMS survival of alleles targeting the conserved zinc hook cysteines, were also comparable to *rad50Δ*.

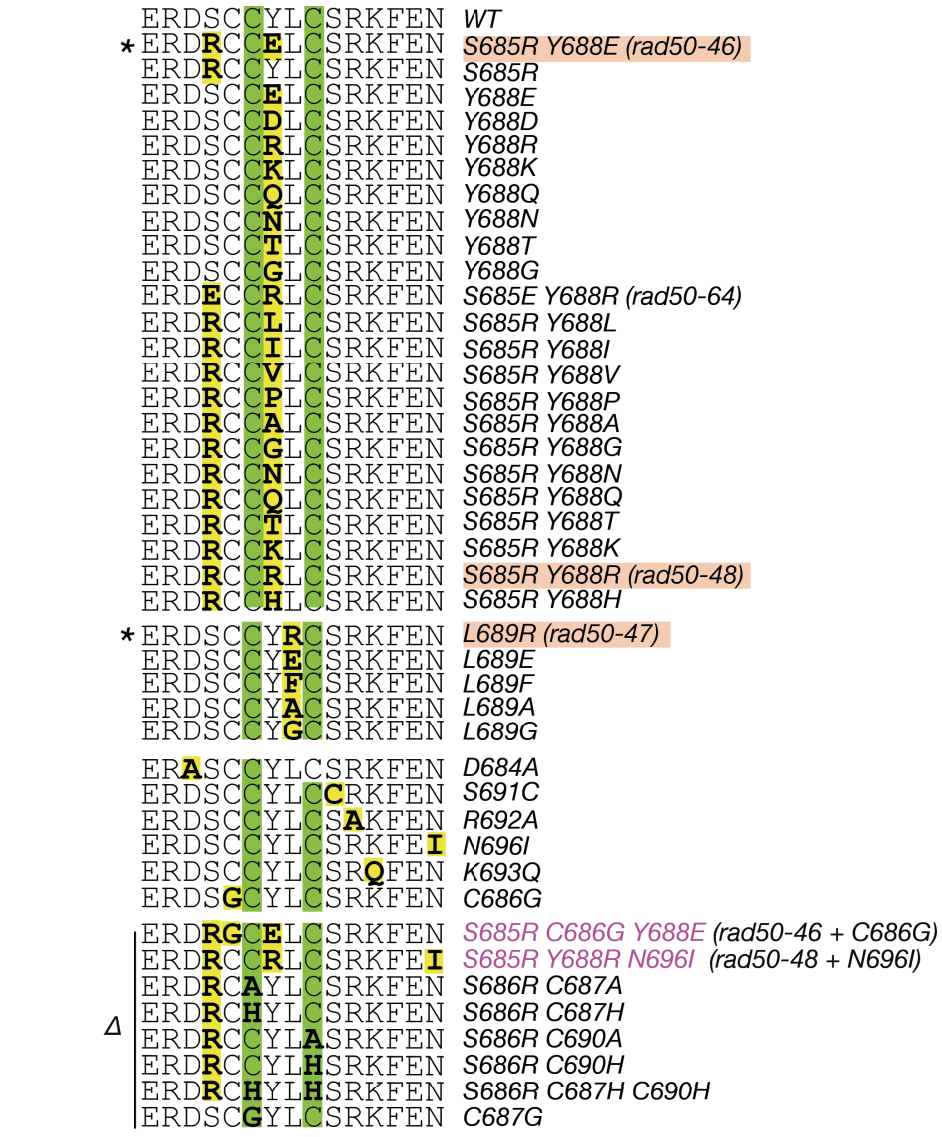


* Partial MMS sensitivity

*Δ* *rad50Δ*-alike MMS sensitivity

unmarked *WT*-alike (no or residual MMS sensitivity)

**Table S3, related to Figure 2 and Experimental Procedures**. Sequences of zinc hook peptides used for steady-state fluorescence anisotropy measurements. 5-CF denotes 5-carboxyfluroescein moiety.

```
Rad50-wt: (5-CF)-KTALENLKMHQTTLEFNRKALEIAERDSCCYLCSRKFENESFKSKLLQELKTKTDANFEKTLKDTVQN-(amide)
Rad50-46: (5-CF)-KTALENLKMHQTTLEFNRKALEIAERDRCCELCSRKFENESFKSKLLQELKTKTDANFEKTLKDTVQN-(amide)
Rad50-47: (5-CF)-KTALENLKMHQTTLEFNRKALEIAERDSCCYRCSRKFENESFKSKLLQELKTKTDANFEKTLKDTVQN-(amide)
Rad50-48: (5-CF)-KTALENLKMHQTTLEFNRKALEIAERDRCCRLCSRKFENESFKSKLLQELKTKTDANFEKTLKDTVQN-(amide
```

**Table S4, related to Figure 2, Figure 7 and Experimental Procedures.** Sequences of zinc hook peptides used in CD and UV absorbance titration experiments.

```
Rad50-wt:        (Acetyl)-LEFNRKALEIAERDSCCYLCSRKFENESFKSKLLQELKTKT-(amide)
Rad50-46:        (Acetyl)-LEFNRKALEIAERDRCCELCSRKFENESFKSKLLQELKTKT-(amide)
Rad50-46-I680V:  (Acetyl)-LEFNRKALEVAERDRCCELCSRKFENESFKSKLLQELKTKT-(amide)
Rad50-46-K700Q:  (Acetyl)-LEFNRKALEIAERDRCCELCSRKFENESFQSKLLQELKTKT-(amide)
Rad50-46-L703F:  (Acetyl)-LEFNRKALEIAERDRCCELCSRKFENESFKSKFLQELKTKT-(amide)
Rad50-47:        (Acetyl)-LEFNRKALEIAERDSCCYRCSRKFENESFKSKLLQELKTKT-(amide)
Rad50-48:        (Acetyl)-LEFNRKALEIAERDRCCRLCSRKFENESFKSKLLQELKTKT-(amide)
```

**Table S5, related to Figure 2, Figure 7 and Experimental Procedures**. The chemical components of zinc buffers used in this study and related free $Zn^{2+}$ concentration values.

| **Competitor** | **Total $Zn^{2+}$ (mM)** | **Free [$Zn^{2+}$]** | **-log[$Zn^{2+}$]** |
|---|---|---|---|
| 1.0 mM EDTA | 0 | - | - |
| 1.0 mM HEDTA | 0.2 | $1.64 \times 10^{-13}$ | 12.79 |
| 1.0 mM HEDTA | 0.4 | $4.36 \times 10^{-13}$ | 12.36 |
| 1.0 mM HEDTA | 0.6 | $9.81 \times 10^{-13}$ | 12.01 |
| 1.0 mM HEDTA | 0.8 | $2.62 \times 10^{-12}$ | 11.58 |
| 1.0 mM EGTA | 0.05 | $3.57 \times 10^{-11}$ | 10.45 |
| 1.0 mM EGTA | 0.1 | $7.54 \times 10^{-11}$ | 10.12 |
| 1.0 mM EGTA | 0.3 | $2.91 \times 10^{-10}$ | 9.54 |
| 1.0 mM EGTA | 0.5 | $6.78 \times 10^{-10}$ | 9.17 |
| 1.0 mM EGTA | 0.9 | $6.11 \times 10^{-9}$ | 8.21 |

## Supplemental Experimental Procedures

### Yeast Experiments, Western and Southern blots

All gene replacements and knockouts were done in diploid cells and dissected spores were verified by PCR genotyping and sequencing. In some experiments, Rad50 was also expressed in haploid or diploid *rad50Δ* cells from the single copy centromeric plasmid *Ycp50* (*URA3)* under control of its native promoter. Strains were either grown in YPD or synthetic dropout medium containing 2% glucose. Galactose induction was done as described previously (Hohl et al., 2011). *Ycp50-rad50 Sac*I digested plasmid used for gap repair was gel purified and extracted using QIAprep Spin columns (Qiagen). *rad50-46* suppressor plasmids were rescued from yeast cells according to a protocol specified (Balestrini et al., 2013).

In DNA damage survival assays, cells were grown at 30°C to exponential phase, serially 5-fold diluted and were spotted (250,000 to 80 cells) onto freshly prepared YPD or selective plates containing the indicated concentrations of MMS, CPT or HU. Incubation times varied based on incubation temperatures, and were 2.5-3.5 days at 30°C, 3.5-5 days at 23°C and 1.5-2 days at 37°C. All experiments were performed at least in triplicate with two or more independent diploids or spores.

Nitrocellulose membranes for western blots were incubated with primary and secondary antibodies at room temperature. FLAG-Rad53 phosphorylation was assessed as previously described (Al-Ahmadie et al, 2014) by exposing exponential growing cells for 90 min to 0.1% MMS.

SK1 strains were cultivated and genomic DNA was prepared essentially as described (Murakami et al., 2009), but including an additional phenol chloroform extraction following proteinase K treatment.

For southern blotting, agarose gels were denatured in 0.5M NaCl and 0.5M NaOH and transferred oN by capillary transfer on Amersham Hybond-XL membrane (GE Healthcare). Meiotic DSB formation and repair by meiotic recombination was measured in strains containing the *HIS4::LEU2-(BamHI)/his4-X::LEU2-(NgoM IV)-URA3* heteroalleles (Hunter and Kleckner, 2001). Briefly, XhoI digested genomic DNA was separated on a 0.6% agarose gel and the membrane hybridized with 0.5 kb probe A (3′ end of *STE50* open reading frame) generated by PCR with primer *STE50-1F* (GGTGTGTCTCTTTCACAAACAG) and *STE50-1R* (CTTCCACCGGGGGTGAC). Meiotic intragenic recombination frequencies of *his4B*/*his4X* heteroalleles were determined by return to growth experiments as described (Cao et al., 1990). Telomeres were detected by Southern blot with *Pst*I-digested genomic DNA and a telomere-specific probe (5′-TGTGGTGTGTGGGTGTGGTGT-3′) as described (Hohl et al., 2011).

### Fluorescence anisotropy, UV titration and CD spectroscopy

Peptides of 41 or 68 amino acids in lengths were synthesized on solid phase using Fmoc strategy in microwave-assisted automated peptide synthesizer (CEM Liberty 1) and purified by RP-HPLC as previously reported (Pomorski et al., 2013). In case of 68-mer peptides, solid

phase synthesis was combined with native chemical ligation (Blanco-Canosa and Dawson, 2008). Peptides were N-terminally labeled with 5-carboxylfuorescein (68-mers) or acetylated (41-mers), and C-terminally amidated. Steady state fluorescence anisotropy measurements were performed at 20°C or 30°C using 5-carboxyfluorescein labeled 68-mer peptides at a final concentration of 50 nM incubated in a series of metal-buffers controlling free $Zn^{2+}$ containing 50 mM HEPES pH 7.4, 100 mM NaCl, 30 μM TCEP, 1 mM chelator (EDTA, HEDTA or EGTA) and $ZnSO_4$ in the range of 0 - 0.9 mM (see Supporting Information). UV absorbance and circular dichroism (CD) measurements were performed at 20 °C with non-fluorescently modified (acetylated and amidated only) 41-mers. Peptides at a concentration of 5 μM were titrated with $ZnSO_4$ in 50 mM borate buffer pH 7.4, 100 mM $NaClO_4$, 60 μM TCEP using 1.0 cm-path length cuvette.

***Preparation of metal buffers and steady-state fluorescence anisotropy studies of 68-mer peptides.***

The $Zn^{2+}$ depended dimerization of 5-carboxyfluorescein labeled 68-mer zinc hook peptides (Table S3) was monitored by steady state fluorescence anisotropy measurements in a series of metal buffers (Table S5).

***Preparation of metal buffers:***

Briefly, 1 mM concentration of appropriate $Zn^{2+}$ chelator (EDTA, HEDTA or EGTA) was used with various concentrations of $ZnSO_4$ (0 - 0.9 mM) in 50 mM HEPES, 100 mM NaCl, 60 uM TCEP at pH 7.4 to maintain the free $Zn^{2+}$ concentration at a constant nano- (EGTA) or subnano- and pico- (HEDTA) molar level (Table S4). Additionally, chelator-only (1mM EDTA) buffer without $ZnSO_4$ was used. Accurate free $Zn^{2+}$ values were calculated based on protonation constants of HEDTA ($\beta_{HL} = 9.81$, $\beta_{H_2L} = 15.18$, $\beta_{H_3L} = 17.78$), EGTA ($\beta_{HL} = 9.4$, $\beta_{H_2L} = 18.32$, $\beta_{H_3L} = 20.98$, $\beta_{H_4L} = 22.98$ ) and their stability constants with Zn(II) ($\beta_{ZnL}^{HEDTA} = 14.6$, $\beta_{ZnL}^{EGTA} = 12.7$, $\beta_{ZnHL}^{EGTA} = 17.66$) using the program HySS2009 (Table S4). (Martell and Smith, 1974; Alderighi et al, 1999)

***Steady-state fluorescence anisotropy measurements***

Steady-state fluorescence anisotropy measurements were obtained using a Jobin Yvon Fluoromax-3 spectrofluorimeter (Horiba) equipped with Peltier-thermostatted cell holder. The excitation and emission wavelengths were set to $\lambda_{ex}$ = 492 nm and $\lambda_{em}$ = 520 nm. 5-carboxyfluorescein labeled peptides at a final concentration of 50 nM were incubated for 48h at 20°C in a series of metal buffer prior to measurement at 20°C. Afterwards, the samples were incubated for further 4h at 30°C and then measured again at 30°C.

## Supplemental References


Alderighi L., Gans P., Ienco A., Peters D., Sabatini A. and Vacca A. (1999). Hyperquad simulation and speciation (HySS): a utility program for the investigation of equilibria involving soluble and partially soluble species. Coordination Chemistry Reviews, 184: 311-318.

Cao, L., Alani, E., and Kleckner, N. (1990). A pathway for generation and processing of double-strand breaks during meiotic recombination in S. cerevisiae. Cell *61*, 1089-1101 issn: 0092-8674.

Hunter, N., and Kleckner, N. (2001). The single-end invasion: an asymmetric intermediate at the double-strand break to double-holliday junction transition of meiotic recombination. Cell *106*, 59-70.

Martell E. and Smith R. M. (1974). Critical Stability Constants.
(Plenum Press, New York).

Murakami, H., Borde, V., Nicolas, A., and Keeney, S. (2009). Gel electrophoresis assays for analyzing DNA double-strand breaks in Saccharomyces cerevisiae at various spatial resolutions. Methods in molecular biology *557*, 117-142.